RSC Advances

ROYAL SOCIETY
OF CHEMISTRY

www.rsc.org/advances

ARTICLE TYPE

A simple one pot synthesis of cubic Cu_5FeS_4

Prashant Kumar[a], Meenakshi Gusain[a], Pandian Senthil Kumar[b], Sitharaman Uma[a] and Rajamani Nagarajan[a]*

Reaction of CuCl, FeCl$_3$ and thiourea in ethylene glycol under refluxing conditions yielded micro flower shaped cubic Cu$_5$FeS$_4$ as confirmed from high resolution PXRD, SEM with EDX, UV-Visible, Raman spectroscopy and magnetic
10 **measurements at room temperature.**

In addition to embracing a special status among copper-age minerals, and serving as copper ore, compositions belonging to Cu-Fe-S family exhibit interesting properties ranging from earth science to advanced functional materials. Presence of both Cu
15 and Fe in the same crystal lattice imparts tuneable electrical and magnetic properties such as dilute magnetic semiconducting (DMS) behaviour[1]. Additional control of properties can be achieved by varying the chemical composition/structural arrangements.[2, 3] Since both the metal ions present in Cu-Fe-S are
20 earth abundant, they are projected to be low cost alternative for various I-III-VI systems (such as Cu-In-S, Cu-Ag-S, Ag-In-S, Ag-Ga-S). CuInS$_2$ shows band gap of 1.5 eV in the visible region and therefore have been extensively studied as photovoltaic materials. On the other hand, the optical band gap for CuFeS$_2$
25 (0.6 eV) does not lie in the range suitable for photovoltaic applications and coerced reasearchers to explore and identify other compsoitions in Cu-Fe-S system, whose band gap is suitable to be used as photovoltaic materials. Plass and co-workers reported the optical band gap of nano particles of
30 Cu$_5$FeS$_4$, obtained by the reaction of Cu(acac)$_2$, Fe(acac)$_3$, and elemental S in dodecanethiol and oleic acid,[4] to be 1.25 eV for the first time. However, bulk solution phase synthesis of Cu$_5$FeS$_4$ is essential to further study their properties as well as to examine their photovoltaic functions. To the best of our knowledge, except
35 the report of Plass and coworkers, synthesis reports for Cu$_5$FeS$_4$ are mostly indirect by copper enrichment or by the solid state reaction of binary sulphides at high tempeatures for longer durations.[5-7] Existence of large number of chemical compositions, unquenchable (and even moderate) temperature phases, presence
40 of the metal ions, that can show variable oxidation states; and significant difference in chalcophilic character of Cu and Fe, might be the major hurdles behind the less exploration of synthetic strategy for Cu-Fe-S compositions in general and Cu$_5$FeS$_4$ in particular.[8,9] Specific composition targeted synthetic
45 strategy in desired symmetry in Cu-Fe-S system is still a challenging task. Additional difficulty arises from the polymorphic arrangements existing in Cu$_5$FeS$_4$ (as high, intermediate, and low bornite). The high-temperature polymorph

possesses antifluorite-type structure, consisting of a random
50 distribution of six metal cations and two vacancies in the eight tetrahedral interstices of a cubic close-packed sulphur framework and such an arrangement is stable above 270°C.[10-13] Based on the single crystal data, Morimoto[10,11] has reported that cubic symmetry of Cu$_5$FeS$_4$ results from the twinning of domains with
55 rhombohedral symmetry in eight different orientations. In this rhombohedral structure, all the metal atoms are positioned in three out of four tetrahedral units in a cubic close packed sulphur sub-lattice as in the case of rhombohedral Cu$_9$S$_5$ (Cu$_{1.8}$S).[12,13]The intermediate and low forms can be described as superstructures of
60 the high temperature cubic form due to increase in the ordering of vacancies and the metal atoms with reducing temperature.[14-16]

Given these complexities, phase selective, direct, reproducible, rapid and one-pot synthesis of Cu$_5$FeS$_4$ is justified. As cubic Cu$_5$FeS$_4$ and rhombohedral Cu$_9$S$_5$ (Cu$_{1.8}$S) phases
65 exhibit almost similar kind of atomic and vacancy ordered arrangements, it can be conceptually conceived that a solution based synthetic strategy producing Cu$_9$S$_5$ (Cu$_{1.8}$S)[17] reliably and reproducibly may be suitable for easy stabilization of Cu$_5$FeS$_4$ based on the kinetics and energy considerations. Also, it can be
70 conceived that if ionized iron species can be introduced during the formation of Cu$_9$S$_5$ (Cu$_{1.8}$S), probability of inclusion of iron in it will be quite high. Following our extensive research on copper sulphides and copper containing ternary sulphides,[3, 17-21] it was quite clear that Cu$_9$S$_5$ can be easily realized from the reaction
75 of copper salts with thiourea in ethylene glycol and therefore the introduction of iron during its formation leading to Cu$_5$FeS$_4$ has been studied and the results are reported in this communication.

0.50 g (5 *mmol*) of freshly prepared CuCl, 0.81 g (5 *mmol*) FeCl$_3$ (Thomas Baker, 99%) and 0.76 g (10 *mmol*) thiourea (SRL,
80 98%) were refluxed together in ethylene glycol (100 mL) for 1.5 h. After the reaction, product in the form of suspension was separated by centrifugation. Finally, it was washed several times with d.d. water, absolute alcohol and CS$_2$. It was dried at room temperature. The phase composition and structure of the final
85 products were examined from powder X-ray diffraction patterns using a Bruker D8 Discover X-ray diffractometer employing Cu K$_\alpha$ radiation (λ = 1.5418 Å) with a scan rate of 1.2 s/step and step size 0.02° at 298 K. Raman spectra of the samples, in compact form, were collected using a Renishaw spectrophotometer
90 equipped with a microscope and operating with a laser of wavelength 514 nm. Magnetic measurements were carried out at 300 K using a Vibrating Sample Magnetometer (Microsense

EV9). Transmission Electron Microscopy (TEM) and Selected Area Electron Diffraction (SAED) were carried out using FEI Technai G^2 20 electron microscope operating at 200 kV. The morphology and elemental mapping of the final products was examined from SEM images obtained using FESEM, FEI Quanta 200F microscope equipped with EDX accessories. UV-Visible diffuse reflectance data of the samples were collected over the spectral range of 200-1000 nm using a Perkin Elmer Lamda 35 scanning double-beam spectrometer equipped with a 50 mm integrating sphere. Photoluminescence (PL) measurements were performed on a Horiba Jobin Yvon Fluorolog 3 Spectrofluorometer at room temperature.

In the PXRD pattern of the product from the reaction of CuCl, FeCl$_3$ and thiourea in ethylene glycol, sharp reflections in the 2θ range of 10-70° were observed indicating high crystalline nature of the samples (Fig. 1 (a)). The presence of less number of reflections suggested the product to possess higher symmetry. The shift of the observed reflections towards higher 2θ values with respect to Cu$_9$S$_5$ (Cu$_{1.8}$S) indicated possible inclusion of additional cation in it. Further, search-match of the JCPDS data base for high symmetry compositions consisting of Cu, Fe and S yielded a close match with Cu$_5$FeS$_4$ (JCPDS file no. 34-0135) and therefore the observed peaks were indexed in cubic symmetry (space group *Fm3m* (#225)) with lattice constant of *a* = 10.98 Å.[13] Of the many fundamental problems on the super structure of bornite, Fe/Cu ordering plays a significant and decisive role on the final ordering present in the samples. Based on magnetic struture, TEM studies coupled with first principle calculations, two Fe/Cu ordering schemes indicating the filling of Fe in the tetrahedral sites of sulphur atoms in the antifluroite cube and the vacancies at the copper positions having zincblende cube of the supperstructure have been found to exist in Cu$_5$FeS$_4$.[13] A difference in energy of 52.7 meV/unitcell have been computed between these two ordering.[13] As Fe and Cu exhibit similar X-ray and electron scattering factors, the unequivocal assignment of the observed phase as Cu$_5$FeS$_4$ and not Cu$_9$S$_5$ may not be absolutely ceratin eventhough the observed peak at higher 2θ (around 69°) is observed only for Cu$_5$FeS$_4$. Therefore, additional evidence has been gathered from Raman spectroscopy measurements. The sample showed one strong peak at 472 cm^{-1} (shown in Fig. 1(b)) in the Raman spectrum[23]. However, on deconvolution, the presence of two bands at 465 cm^{-1} and 472 cm^{-1} was evident (inset of Fig. 1(b)). Such a deconvolution was not observed in the Raman spectrum of Cu$_9$S$_5$ (Fig.S3 †ESI). This was a crucial evidence for the formation of Cu$_5$FeS$_4$.

A low magnification FESEM image of Cu$_5$FeS$_4$ is presented in Fig. 2(a) showing uniform flower like structure with an average diameter of 10 µm. In the selected area electron diffraction (SAED) pattern recorded from the high resolution TEM showed well defined spots that were indexed corresponding to [800], [444], [440], [331], [311] planes of the cubic cell (inset of Fig. 2 (a)). On higher magnification, micro-flower morphology consisting of a hierarchical structure was observed (Fig. 2(b)). The nanosheets intersected with each other resulting in a net like structure with porous surfaces. Interestingly, 3D flower structures were assembled by a large number of nanosheets with an average microflower morphology have earlier been observed for CuS and SnS$_2$ obtained in ethyleneglycol and polyethyleneglycol,

respectively [17, 24]. It is therefore reasoanble to state that ethylene glycol solvent system used in the current study obtained microflower morphology may be The emission spectrum of the sample at an excitation wavelength of 500 nm showed low intense signal centered at 750 nm, such emission characteristics were not observed or reported earlier for Cu-S compositions
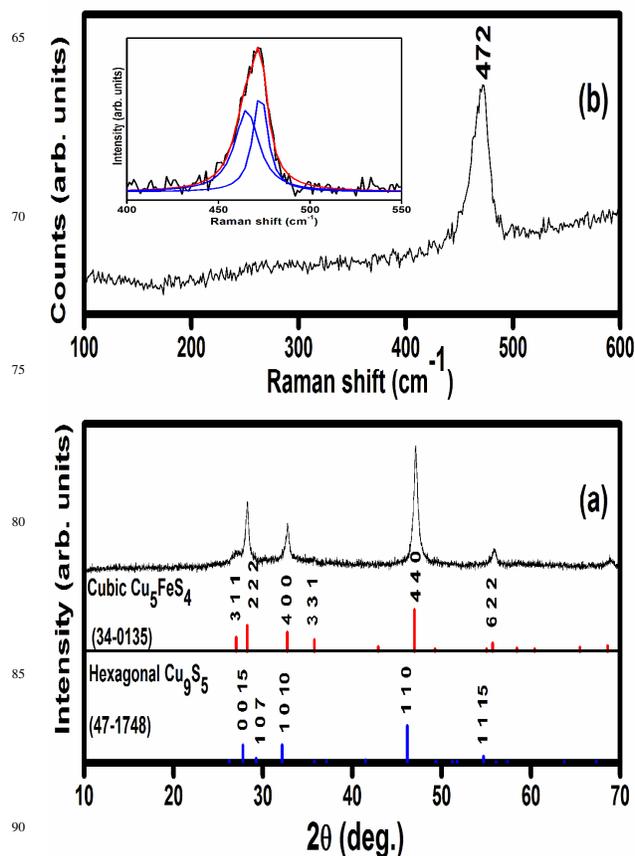
Fig.1 (a) PXRD pattern of the product, obtained by reaction of CuCl, FeCl$_3$ and thiourea in ethylene glycol for 1.5 h. and (b) Raman spectrum of Cu$_5$FeS$_4$ obtained in the present set of reactions. Inset in (b) shows the deconvolution of the Raman spectrum. JCPDS cards for Cu$_5$FeS$_4$ and Cu$_9$S$_5$ (Cu$_{1.8}$S) are provided for easy comparison.
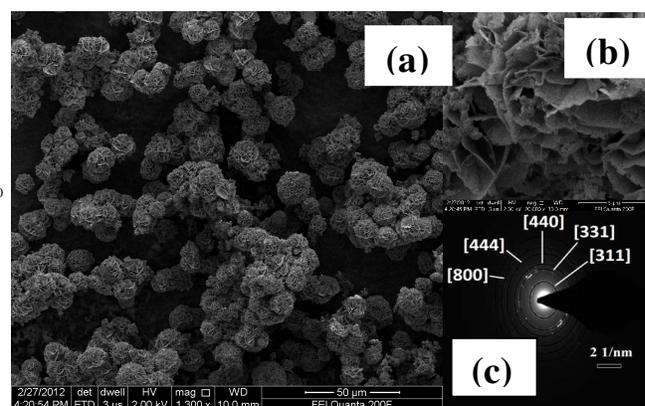
Fig.2 (a) and (b) show the low and high magnification FESEM image with EDX analysis of cubic Cu$_5$FeS$_4$. Indexed SAED pattern from the TEM experiments is shown in (c).

thickness of 14 nm. EDX analysis of the sample revealed Cu: Fe: S as 4.9: 1.4: 3.8, closely matching with the expected ratio between copper, iron and sulphur (inset of Fig. 2(b)). Such (inset of Fig. 3(a)). However, emissions in this range are usually observed for non-stoichiometric copper containing I-III-VI$_2$ compounds,[22,25] thereby suggesting the possibility of iron
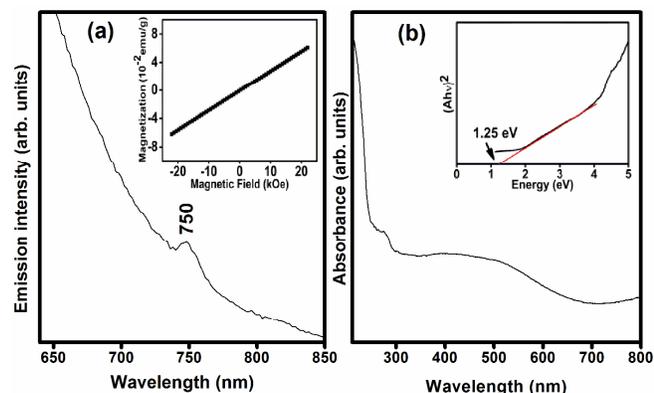
Fig.3 (a) and (b) show photoluminescence emission obtained with λ_{exc} = 500 nm and UV-Visible absorbance spectrum spectrum of Cu$_5$FeS$_4$, respectively. Plot of magnetic field versus magnetization and plot of photon energy (eV) Vs $(\alpha h\nu)^2$ are shown in the insets of (a) and (b), respectively.

incorporation in the Cu-S system. Paramagnetic behaviour of the sample (inset of Fig. 3(a)), observed at room temperature also offered additional support for the presence of magnetic Fe^{3+} ion in the sample. Copper sulphide (Cu$_x$S) compositions are known to show weak paramagnetism only for x =1-1.12[17]. Also, iron sulphide compositions, synthesized by the reaction of FeCl$_3$ with thiourea were reported to exhibit ferromagnetic behaviour[25] and not a simple paramagnetic behaviour. From the UV-Visible spectroscopy data (shown in Fig. 3(b)), band gap value of 1.25 eV was deduced for Cu$_5$FeS$_4$, which was quite comparable with the reported value[4].

To answer whether the reaction of other iron salts such as Fe(NO$_3$)$_3$.9H$_2$O or Fe$_2$(SO$_4$)$_3$ with CuCl and thiourea could yield Cu$_5$FeS$_4$ or any other ternary composition, experiments were performed under identical conditions taking them as iron sources. PXRD patterns of the products from these reactions showed the formation of binary sulphides of copper and iron (Fig.S4 †ESI). These results hinted regarding the possible mechanism of formation of copper rich Cu$_5$FeS$_4$ from the reaction of CuCl, FeCl$_3$ and thiourea. Independent reactions of CuCl with thiourea and FeCl$_3$ with thiourea by polyol process have been reported to yield copper rich Cu$_{1.8}$S and Fe$_3$S$_4$, respectively[26]. The occurrence of these two species in higher symmetry along with the highly cation fluidic character of Cu$_{1.8}$S possibly might have promoted the formation of copper rich cubic Cu$_5$FeS$_4$[27]. Also, the existence of Fe^{2+} and Fe^{3+} in Fe$_3$S$_4$ increases the probability of cation exchange with Cu^{1+} and Cu^{2+} present in Cu$_9$S$_5$ (Cu$_{1.8}$S).

Conclusion

High bornite Cu$_5$FeS$_5$ was synthesized in pure form by adopting a target oriented approach, derived from isostructural binary copper sulphide following a single step and one pot strategy. As the reactions are simple and scalable, they can easily be implemented under industrial conditions for viable applications.

Notes and references

^{a} *Materials Chemistry Group, Department of Chemistry, University of Delhi, Delhi, India. Fax: +91-11-27666605; Tel: 91-11-27662650; E-mail: rnagarajan@chemistry.du.ac.in.*
^{b} *Department of Physics and Astrophysics, University of Delhi, Delhi, India.*

1 K. J. Klabunde, Nanoscale Materials in Chemistry, Wiley Interscience, 2001.
2 L. Barkat, N. Hamdadou, M. Morsli, A. Khelil and J.C. Bernède, *J. Crystal Growth*, 2006, **297**, 426.
3 P. Kumar, S. Uma, and R. Nagarajan, *Chem. Commun.*, 2013, **49**, 7316.
4 A. M. Wiltrout, N. J. Freymeyer, T. Machani, P. Rossi and K. E. Plass, *J. Mater. Chem.*, 2011, **21**, 19286.
5 W. M. B. Roberts, *Econ. Geol.*, 1963, **58**, 52.
6 D. B. Roberts and D. J. Williams, *Mat. Res. Bull.*, 1974, **10**, 163.
7 R. Berger and R. V. Bucur, *Solid State Ionics*, 1996, **89**, 269.
8 P. B. Barton, Jr. *Econ. Geol.*, 1973, **68**, 455.
9 V. Raghavan, *J. Phase Equilib Diffus.*, 2004, **25**, 450.
10 N. Morimoto and G. Kullerud, *Am. Mineral.*, 1961, **46**, 1270.
11 Y. Kanazawa, K. Koto and N. Morimoto, *Canadian Mineral.*, 1978, **16**, 397.
12 N. Morimoto, *Acta Cryst.*, 1964, **17**, 351.
13 Y. Ding, D. R. Weblen and C. T. Prewitt, *Am. Mineral.*, 2005, **90**, 1265.
14 K. Koto and N. Morimoto, *Acta Crystal.*, 1975, **B31**, 2268.
15 L. Pierce and P.R. Buseck, *Am. Mineral.*, 1978, **63**, 1.
16 A. Putnis and J. Grace, *Contrib. Mineral. Petr.*, 1976, **55**, 311.
17 P. Kumar, M. Gusain and R. Nagarajan, *Inorg. Chem.*, 2011, **50**, 3065.
18 P. Kumar and R. Nagarajan, *Inorg. Chem.*, 2012, **50**, 9204.
20 P. Kumar, R. Nagarajan and R. Sarangi, *J. Mater. Chem. C,* 2013, **1**, 2448.
21 P. Kumar, M. Gusain and R. Nagarajan, *Inorg. Chem.*, 2012, **51**, 7945.
22 M. Gusain, P. Kumar and R. Nagarajan, *RSC Adv.*, 2013, **3**, 18863.
23 (a) B., Minceva-Sukarova, M. Najdoski, I. Grozdanov, C. J. Chunnilall, *J. Mol. Struct.*, 1997, **410- 411**, 267; (b) T.P. Mernagh and A. G. Trudu, *Chemical Geology,* 1993, **103**, 113.
24 H. Ke, W. Luo, G. Cheng, X. Tian, and Z. Pi, *Micro & Nano Letters*, 2009, **4,** 177.
25 M. Uehara, K. Watanabe, Y. Tajiri, H. Nakamura and H. Maeda, *J. Chem. Phys.*, 2008, **129**, 134709.
26 D.-G. Lee, N.-H. Lee, H.-J. Oh, S.-C. Jung, J.-S. Hwang, W.- J. Lee and S.-J. Kim, *J. Nanosci. Nanotechnol.*, 2011, **11**, 1434.
25 C. I. Pearce, R. A. D. Pattrick and D. J. Vaughan, *Rev. Mineral. Geochem.*, 2006, **51**, 127.
26 G. Shen, D. Chen, K. Tang, X. Liu, L. Huang and Y. Qian, *J. Solid State Chem.*, 2003, **173**, 232.
27 X. Lu, Z. Zhuang, Q. Peng and Y. Li, *Cryst Eng Comm*, 2011, **13**, 4039